SLC17A6/7/8 Vesicular Glutamate Transporter Homologs in Nematodes

Esther Serrano-Saiz,*,†,1 Merly C. Vogt,* Sagi Levy,‡ Yu Wang,§ Karolina K. Kaczmarczyk,* Xue Mei, Ge Bai,§ Andrew Singson,**,†† Barth D. Grant,§ and Oliver Hobert***

*Department of Biological Sciences, Columbia University, Howard Hughes Medical Institute, New York, New York 10027, †Centro de Biologia Molecular Severo Ochoa/CSIC, Madrid, Spain, ‡Rockefeller University, New York, New York 10065, §Department of Molecular Biology and Biochemistry, **Waksman Institute, and ††Department of Genetics, Rutgers University, Piscataway, New Jersey 08854

ORCID IDs: 0000-0003-0077-878X (E.S.-S.); 0000-0002-5091-0892 (A.S.); 0000-0002-5943-8336 (B.D.G.); 0000-0002-7634-2854 (O.H.)

ABSTRACT Members of the superfamily of solute carrier (SLC) transmembrane proteins transport diverse substrates across distinct cellular membranes. Three SLC protein families transport distinct neurotransmitters into synaptic vesicles to enable synaptic transmission in the nervous system. Among them is the SLC17A6/7/8 family of vesicular glutamate transporters, which endows specific neuronal cell types with the ability to use glutamate as a neurotransmitter. The genome of the nematode *Caenorhabditis elegans* encodes three SLC17A6/7/8 family members, one of which, *eat-4/VGLUT*, has been shown to be involved in glutamatergic neurotransmission. Here, we describe our analysis of the two remaining, previously uncharacterized SLC17A6/7/8 family members, *vglu-2* and *vglu-3*. These two genes directly neighbor one another and are the result of a recent gene duplication event in *C. elegans*, but not in other *Caenorhabditis* species. Compared to EAT-4, the VGLU-2 and VGLU-3 protein sequences display a more distant similarity to canonical, vertebrate VGLUT proteins. We tagged both genomic loci with *gfp* and detected no expression of *vglu-3* at any stage of development in any cell type of both *C. elegans* sexes. In contrast, *vglu-2*::*gfp* is dynamically expressed in a restricted set of distinct cell types. Within the nervous system, *vglu-2*::*gfp* is exclusively expressed in a single interneuron class, AIA, where it localizes to vesicular structures in the soma, but not along the axon, suggesting that VGLU-2 may not be involved in synaptic transport of glutamate. Nevertheless, *vglu-2* mutants are partly defective in the function of the AIA neuron in olfactory behavior. Outside the nervous system, VGLU-2 is expressed in collagen secreting skin cells where VGLU-2 most prominently localizes to early endosomes, and to a lesser degree to apical clathrin-coated pits, the *trans*-Golgi network, and late endosomes. On early endosomes, VGLU-2 colocalizes most strongly with the recycling promoting factor SNX-1, a retromer component. Loss of *vglu-2* affects the permeability of the collagen-containing cuticle of the worm, and based on the function of a vertebrate VGLUT1 protein in osteoclasts, we speculate that *vglu-2* may have a role in collagen trafficking in the skin. We conclude that *C. elegans* SLC17A6/7/8 family members have diverse functions within and outside the nervous system.

KEYWORDS *C. elegans*; neurotransmitter; vesicular transporter

THE solute carrier (SLC) superfamily of transmembrane transporters is subdivided into > 40 families (Hediger *et al.* 2004; Höglund *et al.* 2011). Cellular and subcellular localization and transport substrates are known for many but not all SLC transporters. Three different SLC families package neurotransmitter into synaptic vesicles and, hence, are critical for chemical communication at the neuronal synapse (Hediger *et al.* 2004; Reimer 2013; Omote *et al.* 2016): (1) SLC32 (VGAT) is a vesicular transporter of the inhibitory amino acid transporter family (GABA and glycine); (2) SLC18 family members are vesicular transporters for monoamines (VMAT1/2 = SLC18A1/2) or for acetylcholine (VAChT = SLC18A3); and (3) three members of the SLC17 family of organic anion transporters are vesicular transporters for glutamate (VGLUT1/2/3 = SLC17A6/7/8) (Figure 1, A and B).

The nematode *Caenorhabditis elegans* contains representatives of each of these transporters (Alfonso *et al.* 1993;

doi: https://doi.org/10.1534/genetics.119.302855
Manuscript received October 29, 2019; accepted for publication November 24, 2019; published Early Online November 27, 2019.
Supplemental material available at figshare: https://doi.org/10.25386/genetics.11233499.
[1]Corresponding author: Howard Hughes Medical Institute, 1212 Amsterdam Ave., New York, NY 10027. E-mail: esther.serrano.saiz@gmail.com

McIntire *et al.* 1997; Duerr *et al.* 1999; Lee *et al.* 1999, 2008). The analysis of the expression patterns of *C. elegans VGAT*, *VMAT*, and *VAChT* has been used to define the full complement of GABAergic, aminergic, and cholinergic neurons of the hermaphrodite and male nervous system of *C. elegans* (McIntire *et al.* 1997; Duerr *et al.* 1999, 2001; Pereira *et al.* 2015; Gendrel *et al.* 2016; Serrano-Saiz *et al.* 2017). Similarly, the expression pattern of the *eat-4/VGLUT* gene has identified 38 glutamatergic neuron classes in the hermaphrodite nervous system (Serrano-Saiz *et al.* 2013) and 6 additional neuron classes in the male nervous system (Serrano-Saiz *et al.* 2017). However, 14 of the 118 neuron classes in the hermaphrodite and an additional 14 neuron classes in the dimorphic male nervous system fail to express any known synaptic vesicular transporter, and hence lack an assigned neurotransmitter identity (Serrano-Saiz *et al.* 2017). One possibility that we considered here in this paper is that some of these "orphan neurons" may be glutamatergic, since the *C. elegans* genome contains two previously uncharacterized genes with sequence homology to the SLC17A6/7/8 family of vesicular glutamate transporters (Sreedharan *et al.* 2010; Hobert 2013), which we call *vglu-2* and *vglu-3* (Figure 1B).

We describe here our analysis of the *vglu-2* and *vglu-3* genes. We found that *vglu-3* is the result of a recent gene duplication event and we were not able to detect any expression in any cell type under standard conditions. In contrast, we found that *vglu-2* is expressed in a number of distinct neuronal and nonneuronal tissue types, where it localizes to vesicular structures. We find that removal of *vglu-2* affects the proper function of the neuronal and nonneuronal cell types in which it is expressed.

Materials and Methods

Phylogenetic analysis

Nematode sequences were retrieved from WormBase release WS267. Multiple sequence alignment and phylogenetic trees were generated using T-Coffee (https://www.ebi.ac.uk/Tools/msa/tcoffee/) and the Simple Phylogeny package (using the unweighted pair group method with arithmetic mean clustering approach).

C. elegans mutant and genome-engineered strains

For *vglu-2* and *vglu-3* loss-of-function analysis, we used alleles provided by the *C. elegans* Gene Knockout Consortium—*vglu-2(ok2356)* and *vglu-3(tm3990)*—and from the Million Mutation project (Thompson *et al.* 2013). The alleles from the Million Mutation project were *vglu-2(gk738584)* (isolated from VC40640), *gk625231* (isolated from VC40414), *gk835659* (isolated from VC40829), and *vglu-3(gk765782)* (isolated from VC40694). These VC strains were outcrossed four times with N2 wild-type animals.

gfp-tagged *vglu-2* and *vglu-3* gene reporters, *vglu-2 (syb362[vglu-2::gfp])* and *vglu-3(syb679[vglu-3::gfp])*, were generated via clustered regularly interspaced short palindromic repeats (CRISPR)/Cas9 genome engineering by SunyBiotech (Fuzhou, China). The *gfp* cassette from the pDD282 plasmid (Dickinson *et al.* 2015) was engineered right before the stop codons of *vglu-2* and *vglu-3*. The *vglu-2prom2*::*NLS*::*tagrfp* promoter construct (pOH596) contains 2 kb upstream of the *vglu-2* locus (5′-CCAGACATGGGAAACACCTCCATATTTAT[.....]GCTATCTCAAAAAAGTACAAAACGTCCACAA-3′) and was injected into *him-5* animals with *unc-122*::*gfp* as the injection marker (*otEx7346*).

A list of all strains is provided in Supplemental Material, Table S1.

Transgenic strains

To rescue the cuticle fragility assay, the *vglu-2* fosmid reporter was generated by fosmid recombineering using fosmid WRM0628dA10 and an SL2-based, nuclear-localized *yfp* reporter (Tursun *et al.* 2009). Two lines were generated, *otEx7350* and *otEx7351*, by injecting the fosmid reporter at 5 ng/μl into *vglu-2(gk625231)* mutant animals with *unc-122*::*gfp* as injection marker (5 ng/μl). Next, 90 ng/μl of OP50 genomic DNA was added as filling DNA.

To rescue the AIA behavioral defects, *vglu-2* complementary DNA (cDNA) was cloned under the control of a 331-bp *mgl-1* promoter fragment (−1704 to −1374 from ATG) with restricted expression to AIA and NSM neurons (Zhang *et al.* 2014). Two lines were generated, *otEx7407* and *otEx7408*, by injecting the constructs at 5 ng/μl. *myo-2*::*mCherry* was used as a co-injection marker (20 ng/μl), supplemented with 75 ng/μl of pBlueScript plasmid.

To express vesicular markers in the epidermis, single-copy miniMos transgenes were generated (Frøkjær-Jensen *et al.* 2014). cDNAs or genomic DNA for each marker was cloned into a customized version of miniMos vector pCFJ910, including the hyp7-specific promoter from gene *Y37A1B.5*, red fluorescent protein (RFP) wrmScarlet-I (mScarlet), and the 3′-UTR from the gene *let-858* (El Mouridi *et al.* 2017; Köhnlein *et al.* 2019). Markers expressed included SNX-1 (early endosome, retromer-recycling microdomain), HGRS-1 (early endosome, ESCRT-degradative microdomain), RAB-7 (late endosome and lysosome), APM-1 (*trans*-Golgi network), APM-2 (clathrin-coated pit), and LGG-1 (autophagosome).

A list of all transgenic strains is provided in Table S1.

Brood sizing

Brood sizing was conducted as previously described (Singson *et al.* 1998; Geldziler *et al.* 2011; Chatterjee *et al.* 2013). L4-stage hermaphrodites were picked individually onto a one-spot plate at 20°. They were then transferred to a new plate daily until they stopped producing progeny. Progeny were counted 3 days after the hermaphrodite was transferred and total brood size was calculated by adding all the progeny counts from a hermaphrodite.

Sperm activation

Sperm activation was conducted as previously described (Shakes and Ward 1989; Singaravelu *et al.* 2011). L4-stage males were picked onto a plate and separated from

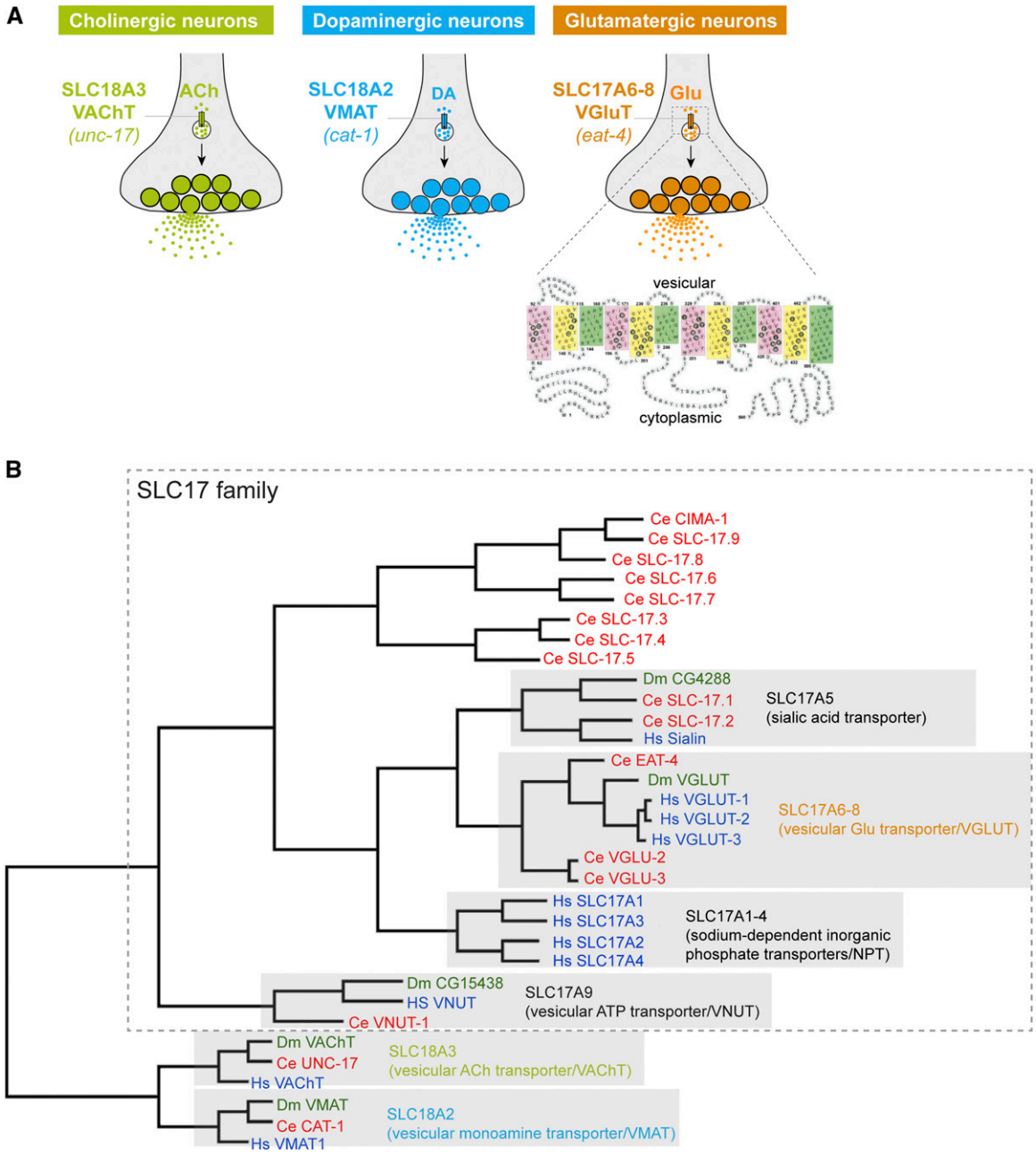

Figure 1 Dendrograms of SLC family members. (A) Several SLC superfamily members are vesicular neurotransmitter transporters whose expression defines specific neurotransmitter identities. The schematic protein structure from human VGLUT1 is from Almqvist *et al.* (2007). ACh, acetylcholine; DA, dopamine; Glu, glutamate; VAChT, vesicular acetylcholine transporter; VMAT, vesicular monoamine transporter; VGluT, vesicular glutamate transporter. (B) Dendrogram of SLC17 family members in *C. elegans*, rooted with members of the SLC18 neurotransmitter transporter families from worms (Ce), flies (Dm), and humans (Hs). While the inclusion of all SLC17 family members weakens the association of VGLU-2 and VGLU-3 with *bona fide* VGLUT proteins (compare to (B)), they still remain more closely associated with VGLUTs compared to other vesicular transporters. SLC, solute carrier.

hermaphrodites at 20° for overnight incubation. Males were then dissected in sperm media (pH 7.8) with or without pronase (200 μg/ml). DIC images of spermatids were taken with a Zeiss ([Carl Zeiss], Thornwood, NY) Universal microscope with a ProgRes camera (Jenoptik) and ProgRes software.

Cuticle fragility assay

Assays were done as previously described (Loer *et al.* 2015). Synchronized 2-day adult animals were placed in a 15 μl drop of hypochlorite solution [5% sodium hypochlorite (household bleach) and 1 M NaOH in H_2O]. Five individual drops with 10 animals (a total of 50 worms) were monitored and the time when the worms exploded was annotated. If > 2 experimental groups were compared, statistical significance was determined using a Kruskal–Wallis test, with a subsequent Dunn's test for multiple comparisons. The Mann–Whitney test was used when two experimental groups were compared.

Cuticle barrier assay

The assay was performed as previously described (Hirani *et al.* 2016). Briefly, synchronized 2-day adult animals were incubated in M9 buffer containing 0.1% (w/v) gelatin and Hoechst 33258 (10 μg/ml) for 15 min at room temperature. Subsequently, the animals were washed twice in M9 containing 0.1% (w/v) gelatin and imaged (40×) immediately. An animal was scored as "stained" if more than six nuclei were clearly visible in the tail region with DAPI staining. In each of the three independent experiments, ∼50 animals were scored for each strain. Statistical significance was determined using one-way ANOVA followed by a *post hoc* Tukey test.

Hypoosmotic sensitivity assay

The assay was performed as previously described (Hirani *et al.* 2016), with few minor changes. For each strain, 24 animals were transferred to 2 ml of distilled water with three animals per well of a 24-well plate. The behavior of each animal was assessed 5, 20, and 40 min after transfer and scored as "mobile," "immobile," "rod-like," or "exploded" for each time point. The assay was performed three independent times for each genotype.

Odor response assays

Microfluidic designs and fabrication, image analysis, and behavior segmentation were done as previously described with small changes (Chronis *et al.* 2007; Albrecht and Bargmann 2011; Levy and Bargmann 2019). Briefly, the device consisted of four separate arenas, allowing simultaneous monitoring of 15 free-moving animals per arena. Two arenas that allowed fast switches between two input channels [controlled by flow channels, modified from Chronis *et al.* (2007)] were used in this study. Hamilton Modular Valve Positioner eight-way valves were located upstream of the microfluidic chamber input channels, allowing the introduction of various odor changes to the animals. Animals were monitored at 6 Hz, and image analysis and behavior segmentation were done using a custom-made MATLAB program (MathWorks). The animal morphologies, trajectories, and head coordinates were extracted and used to identify behavioral states, including forward, reverse, pause, and the stereotypical ω state. In each experiment, 1-day adult animals were exposed to three sequential exposures of diacetyl (2,3-butanedione, product 11038; Sigma [Sigma Chemical], St. Louis, MO) at a particular concentration for 2 min each, separated by 2 min, followed by a similar series at the next higher concentration after a 5-min rest time. Behavior was scored at the time immediately following odor removal. Dye test was performed after each experiment to confirm odor switching quality and to quantify the odor exposure timing of each individual animal. To compute the cumulative probability of reversals (CDF), animals that were not reversing before odor presentation were identified, and the lag between the time of odor removal and the time of reversal initiation was quantified. To compare the CDF in response to removal of diacetyl in concentration A (CDF_A) to the CDF without odor removal (buffer–buffer control, CDF_0) at time t, we defined: $\Delta CDF_A(t) = CDF_A(t) - CDF_0(t)$, and computed its distribution and SD by bootstrap over experimental repeats (Figure 7B and Figure S4 for $A = 1$ μM). The P-value for the hypothesis that $CDF_A(t) > CDF_0(t)$ was extracted from the probability of $\Delta CDF_A(t) < 0$, with false discovery rate (FDR) correction for multiple hypotheses (concentrations, Figure S4). To assess whether $\Delta CDF_A(t)$ calculated for a certain genotype (G) is significantly lower than for wild-type animals, we defined: $\Delta\Delta CDF_{A,G}(t) = \Delta CDF_{A,G}(t) - \Delta CDF_{A,WT}(t)$. The P-value for the hypothesis that $\Delta CDF_{A,WT}(t) > \Delta CDF_{A,G}(t)$ was extracted from the probability of $\Delta\Delta CDF_{A,G}(t) > 0$ in the bootstrap sample, with FDR correction for multiple hypotheses (genotypes, Figure 6B). Results were not sensitive to the choice of statistics, and similar outcomes were obtained when genotypes were compared to wild-type using Kolmogorov–Smirnov (K-S) statistics. Specifically, we defined $\Delta KS_{A,G} = KS_{A,G} - KS_{A,WT}$, where $KS_{A,G}$ is the K-S distance between CDF_A and CDF_0 for genotype G, and represents the maximal vertical distance between the two cumulative distributions, and computed the $\Delta KS_{A,G}$ distribution by bootstrap. The P-value for the hypothesis that $KS_{A,WT} > KS_{A,G}$ was extracted from the probability of $\Delta KS_{A,G} > 0$ in the bootstrap sample, with FDR correction for multiple hypotheses (genotypes), resulting in significant changes for AIA-silenced animals [*Pgcy-28d::unc-103(gf)*, $P < 5 \times 10^{-5}$] and *vglu-2* mutants ($P < 0.05$), but not for rescue strains (*vglu-2;Pmgl-1::vglu-2*).

Microscopy and image analysis

For the colocalization analysis, live first-day adult hermaphrodites were mounted on 2% agarose pads with 10 mM levamisole. Multiwavelength fluorescence colocalization images were obtained using an Axiovert Z1 microscope (Carl Zeiss Microimaging) equipped with a X-Light V2 Spinning Disk Confocal Unit (CrestOptics), a Photometrics Prime 95B Scientific CMOS camera, and a PlanApo 100X/1.46NA oil immersion lens. Data were captured as an image stack with 0.2 μm step size using Metamorph version 7.7 software (Universal Imaging), and deconvolved using Autoquant X3 (Media Cybernetics). In Metamorph, a single plane from each image stack was chosen in which both markers were clearly visible. Images were then thresholded and two hand-drawn regions were designated for each animal, representing the two sides of the epidermis flanking the seam cells. A colocalization coefficient was then calculated for each region using the Correlation Plot application in Metamorph.

Data availability

Mutant and genome engineered strains are available at the Caenorhabditis Genetics Center, others are available upon request. File S1 contains four supplemental figures, supplemental figure legends, and one supplemental table. Supplemental material available at figshare: https://doi.org/10.25386/genetics.11233499.

Results

The SLC17 family in the C. elegans genome

Through reiterative and reciprocal BLAST (Basic Local Alignment Search Tool) searches, we assembled a list of SLC17 family members in *C. elegans* and visualized their sequence relationship via comparative sequence analysis (Figure 1B). Refining and extending previous analyses (Sreedharan *et al.* 2010; Hobert 2013; Shao *et al.* 2013), we found that the *C. elegans* genome codes for orthologs of several SLC17 family members (Figure 1B). These include: (1) the SLC17A6/7/8 subfamily, which encodes well-characterized vertebrate vesicular glutamate transporters (Takamori *et al.* 2000; Liguz-Lecznar and Skangiel-Kramska, 2007), represented by the *C. elegans* *eat-4* gene (Lee *et al.* 1999, 2008); (2) the SLC17A5 subfamily of sialic acid transporters, which may serve as a possible vesicular transporter of aspartate (Miyaji *et al.* 2008) and is represented by two uncharacterized *C. elegans* genes (*slc-17.1* and *slc-17*.2); and (3) the SLC17A9 subfamily, which encodes the vesicular ATP transporter (Sawada *et al.* 2008) and is represented by the also uncharacterized *C. elegans* *vnut-1* gene (Figure 1B). No apparent homologs of type I sodium-dependent inorganic phosphate transporters (SLC17A1 through SLC17A4) appear to be encoded in the *C. elegans* genome. However, the *C. elegans* genome encodes an apparently nematode-specific SLC17-related subfamily that contains eight members with presently unknown transport substrates (Figure 1B) (Sreedharan *et al.* 2010; Hobert 2013). One of them, *cima-1*, is expressed in the epidermis and is required noncell autonomously to control morphological features of adjacent neurons (Shao *et al.* 2013).

Within the SLC17A6/7/8 subfamily of vesicular glutamate transporters, the *C. elegans* genome encodes not only the *bona fide* vesicular glutamate transporter EAT-4 (Lee *et al.* 1999, 2008), but also two proteins with clear sequence similarity to the SLC17A6/7/8 vesicular glutamate transporters, which we named VGLU-2 and VGLU-3 (Figure 1B and Figure 2). Like the canonical, *bona fide* VGLUT transporter EAT-4, VGLU-2 and VGLU-3 contain the charged residues in transmembrane helices 1 and 7 thought to form the so-called "central" glutamate-binding site, elucidated by structural homology modeling (Almqvist *et al.* 2007) (mint arrowheads in Figure 2).

Vertebrate genomes encode three VGLUT proteins—VGLUT-1/SLC17A7, VGLUT-2/SLC17A6, and VGLUT-3/SLC17A8 (Takamori *et al.* 2000, 2001; Gras *et al.* 2002)—but EAT-4, VGLU-2, and VGLU-3 are not one-to-one orthologs of these three vertebrate VGLUT proteins; rather, each set of genes is duplicated independently in the respective lineages (Figure 1B).

VGLUT homologs in other genomes

We examined the origin of the three *C. elegans* VGLUT-encoding genes EAT-4, VGLU-2, and VGLU-3 more closely. Previous analyses (Daniels *et al.* 2004; Horie *et al.* 2008; Abrams and Sossin 2019), as well as our own reciprocal BLAST searches, have revealed that other ecdysozoa (*e.g. Drosophila melanogaster*), lophotrochozoa (*e.g.* molluscs and annelids), echinoderms (*e.g. Strongylocentrotus purpuratus*), and hemichordates (*e.g. Saccoglossus kowalevskii*), as well as primitive chordates (*e.g.* ascidians/urochordates), only contain a single clear VGLUT sequence ortholog. An examination of nematode VGLUT paralogs revealed that while all examined nematode genomes contain a single EAT-4/VGLUT ortholog, the occurrence of additional EAT-4/VGLUT paralogs is variable. Some nematodes, *e.g.*, *Pristionchus pacificus*, contain no VGLUT-encoding gene other than an *eat-4/VGLUT* ortholog. In contrast, all examined *Caenorhabditis* species contain a single *vglu* gene in addition to *eat-4* (Figure 3A). These *Caenorhabditis vglu* genes appear most similar to *C. elegans* *vglu-2*. Similarly, other nematode species, including those from parasitic clade III (*Brugia malayi* and *Onchocerca volvulus*) and clade IV Rhabditidae (*Strongyloides ratti*), also contain only a single *vglu-2*-like gene, in addition to the *eat-4* ortholog that all species contain (Figure 3A).

The *C. elegans* *vglu-2* and *vglu-3* genes are not only very similar to each other (82% sequence identity over the entire length of the encoded proteins; Figure 2), but also directly neighbor one another in the genome (Figure 3B), suggesting that they may have originated via local gene duplication. Examination of syntenic regions in other, well-annotated *Caenorhabditis* genome sequences reveals only a single *vglu* gene in syntenic regions, indicating that the two *C. elegans* *vglu* genes indeed likely arose from a *C. elegans*-specific *vglu-2* gene duplication event (Figure 3B). Even the recently described sister species of *C. elegans*, *C. inopinata* (formerly *C. sp. 34*) (Kanzaki *et al.* 2018) does not display this *vglu* duplication event (J. Rand, personal communication), highlighting the recent nature of this event. This duplication event apparently affected the entire original gene, since both genes are of similar size and contain the full complement of transmembrane domains (Figure 2).

Taken together, our sequence analysis suggests that a single ancestral VGLUT locus duplicated in some, but not all, branches of the nematode lineage and then, within *C. elegans*, duplicated another time, giving rise to a total of three genes. As we will argue below, based on its expression and localization pattern, only EAT-4 may encode a *bona fide* synaptic vesicular transporter of glutamate, consistent with many other invertebrate and simple chordate species containing only a single VGLUT-encoding gene.

C. elegans VGLU-2 is expressed in neuronal and nonneuronal cell types

To examine *C. elegans* VGLU-2 expression and localization, the endogenous *vglu-2* locus was tagged with *gfp* using CRISPR/Cas9 genome engineering. Within the adult nervous system, the resulting strain revealed *gfp* expression in exclusively one bilaterally symmetric neuron pair in the ventral ganglion of the *C. elegans* head in either hermaphrodite or male animals (Figure 4B). By characteristic position and through colabeling with a *cho-1* landmark reporter (*otIs544*), the neuron pair was identified as the AIA interneuron pair

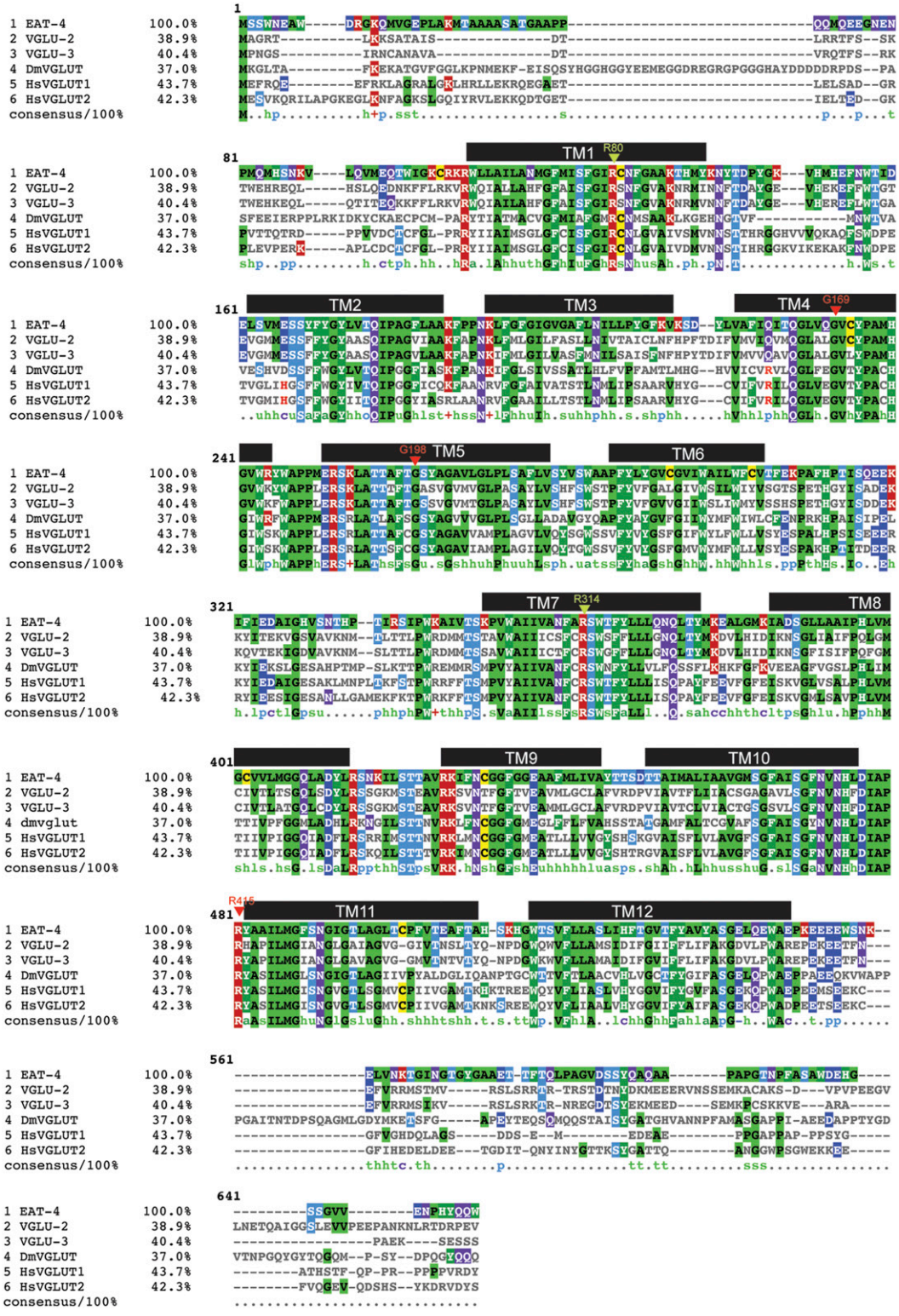

Figure 2 Alignment of VGLUT proteins from various animal species. Sequences of worm, fly, and human VGLUTs. Predicted transmembrane helixes (black bars) are from Almqvist *et al.* (2007). All three *C. elegans* VGLUT proteins contain the predicted central Glu-binding site, defined by R80 and R314 (in VGLUT1 numbering; labeled with mint arrowhead). Red arrowheads indicate the residues mutated in the three missense alleles shown in Figure 6A.

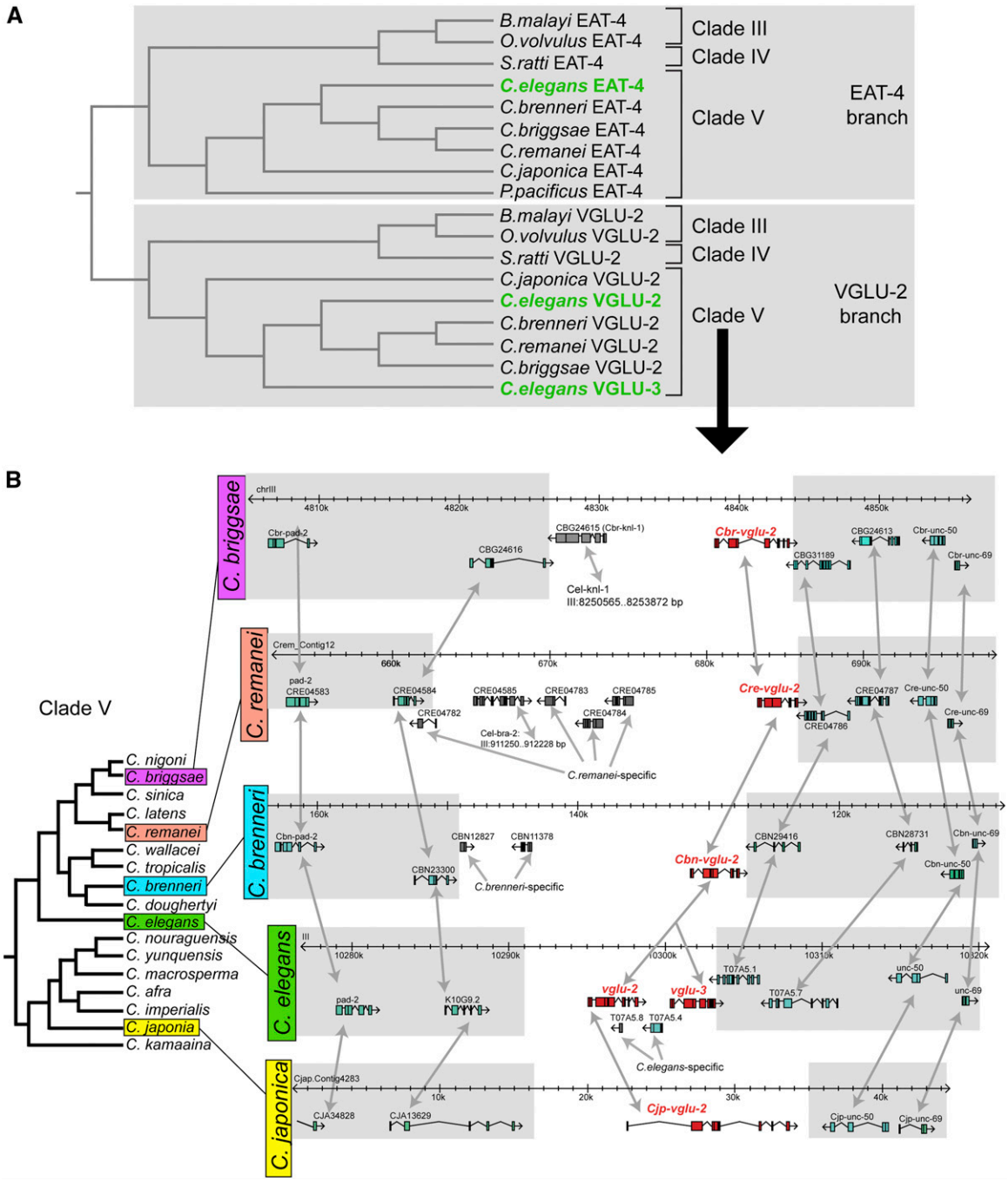

Figure 3 Analysis of VGLUT sequences from different nematode species indicates a *C. elegans*-specific VGLUT duplication. (A) VGLUT homologs in a broad sampling of different nematode species. Clades are according to Blaxter *et al.* (1998). Identifiers are *Strongyloides ratti* genes: EAT-4 = SRP11984; VGLU-2 = SRP11109; for *Onchocerca volvulus* VGLU-2 = OVP03707, and *Brugia malayi* = BM46758. (B) *vglu-2* duplication occurred specifically in *C. elegans*, but not in other Elegans supergroup species. Syntenic genomic intervals from several representative *Caenorhabditis* species from the Elegans supergroup. Gray shading and double-headed arrows indicate synteny. The phylogenetic tree is redrawn from Félix *et al.* (2014). The T07A5.4 gene (erroneously called *ostf-4* in WormBase) that is located between *vglu-2* and *vglu-3* is a *C. elegans*-specific duplicate of the highly conserved F37C4.5 gene located on a different chromosome.

(Figure 4B). The expression in AIA can be observed throughout all larval and adult stages. Expression in males is the same as in hermaphrodites.

Based on the expression of the vesicular transporter for acetylcholine, UNC-17, the AIA interneurons have previously been shown to be cholinergic (Altun-Gultekin *et al.* 2001; Pereira *et al.* 2015). VGLU-2::GFP signals are only observed in the cell body of AIA, not along its axonal process where synaptic contacts are made (Figure 4B). We cannot exclude the possibility that a failure to localize at synapses may be a

consequence of a lack of detection due to very low levels of protein or a reflection of GFP tagging affecting proper protein localization. However, we note that GFP tagging of other SLC-type vesicular neurotransmitter transporters at the C-terminus does not affect their localization or function (McIntire *et al.* 1997; Pereira *et al.* 2015). Moreover, animals with a *gfp* tagged *vglu-2* locus do not exhibit the skin defects that we describe below for *vglu-2* mutants (Figure S2), indicating that GFP tagging does not interfere with VGLU-2 function.

In addition to neuronal expression in the AIA neuron class, we detected prominent *vglu-2*::*gfp* expression outside the nervous system, namely in the syncytial epidermis that covers the entire body (but not the associated seam cells) and in uterine tissue (Figure 4C). In both tissue types, VGLU-2 shows a striking localization to many small puncta. Epidermal cells engage in prominent apical secretion of cuticular proteins (Chisholm and Xu 2012). The V0 subunit of the vacuolar H^+-ATPase (V-ATPase), VHA-5, labels multivesicular bodies that secrete exosomes apically within the epidermis (Liégeois *et al.* 2006; Dierking *et al.* 2011). To assess whether VGLU-2 localizes to these structures, we generated a double transgenic strain of VGLU-2::GFP and RFP-tagged VHA-5, and found that these two proteins do not colocalize (Figure S1).

Collagen turnover also requires endocytosis and endocytic trafficking (Chisholm and Xu 2012). We therefore tested a series of additional organellar markers tagged with RFP, and calculated their relative degree of colocalization using Pearson's Coefficient of Colocalization (Manders *et al.* 1992; Adler and Parmryd 2010) (Figure 5). We found the highest degree of colocalization of VGLU-2::GFP with mScarlet::SNX-1 (Figure 5). SNX-1 is a retromer component that labels the recycling microdomain of early endosomes that directs recycling transmembrane proteins back to the Golgi apparatus, from which they can be resecreted (Norris *et al.* 2017; Zhang *et al.* 2018). We also found significant, but lesser, colocalization with APM-1::mScarlet, a marker for the *trans*-Golgi network; clathrin-coated pit marker mScarlet::APM-2 on the apical surface of the epidermis; mScarlet::HGRS-1, an ESCRT component that marks the degradative microdomain of early endosomes; and tagRFP::RAB-7, a marker for late endosomes and lysosomes (Figure 5) (Sato *et al.* 2014). We also detected a small degree of colocalization with mCherry::UNC-108/Rab2 on sparse large compartments that are also likely to be late endosomes and lysosomes (Lu *et al.* 2008; Yin *et al.* 2017). Finally, we tested mScarlet::LGG-1, a marker for autophagosomes, but found no colocalization with VGLU-2::GFP (Figure 5). Taken together, the VGLU-2::GFP subcellular localization pattern suggests that it may undergo endocytosis from the apical membrane, with a larger fraction recycling from the early endosome to the Golgi, while a smaller fraction is sorted to late endosomes and lysosomes, likely for degradation.

While the expression of VGLU-2::GFP is similar during larval and adult stages in well-fed animals, the expression and localization pattern of VGLU-2::GFP is altered substantially in dauer-stage animals. Expression in the AIA neurons disappears and, in the epidermis, the VGLU-2::GFP expression and localization becomes much weaker and more diffuse (Figure 4D). Upon recovery from the dauer stage, VGLU-2::GFP expression and localization resumes to the state observed in animals that have not passed through the dauer stage. Starvation alone does not affect VGLU-2::GFP expression and localization.

vglu-2 mutants display defects in cuticle function

Four different *vglu-2* mutant alleles were generated by the *C. elegans* Gene Knockout Consortium and the Million Mutation project (*C. elegans* Deletion Mutant Consortium 2012; Thompson *et al.* 2013) (Figure 6A), including one deletion allele *(ok2356)* and three missense alleles that affect completely conserved amino acids within SLC17 family members (red arrowheads in Figure 2).

The localization of VGLU-2 to secretory and endocytic organelles in the epidermis prompted us to examine cuticle integrity in *vglu-2* mutants. The *C. elegans* epidermis is highly secretory in nature and secreted substances include cuticle-building collagens, encoded by $>$ 150 distinct genes in the *C. elegans* genome (Johnstone 2000; Chisholm and Xu 2012). Extracellular collagen matrices are degraded by the proteolytic activity of sodium hypochlorite (Davies *et al.* 1993; Oyarzun *et al.* 2002; Olszowski *et al.* 2003). In fact, sodium hypochlorite treatment ("bleaching") is a standard method to break apart the collagen-containing *C. elegans* cuticle to generate worm lysates (Stiernagle 2006). We tested the susceptibility of *vglu-2* mutants to sodium hypochlorite treatment and found that, compared to wild-type controls, these mutant animals show substantially greater resistance to sodium hypochlorite (Figure 6B). These defects were observed with four different *vglu-2* mutant alleles (Figure 6B). The observed cuticle defect in *vglu-2* mutants was rescued in transgenic animals in which we provided wild-type copies of the *vglu-2* genomic locus on an extrachromosomal array (Figure 6C). This functional readout of *vglu-2* activity also enabled us to ask whether the insertion of the *gfp* tag into the *vglu-2* locus affected gene function in this specific context, and we found this to not be the case (Figure S2). Taken together, we interpret the increased resistance of *vglu-2* mutants to sodium hypochlorite to mean that some aspect of the complex collagen matrix is aberrantly structured in *vglu-2* mutants, which alters the sensitivity of collagens to proteolysis.

To assess the effects of such cuticle changes on one of the major functions of the cuticle, namely its function as a barrier to exogenous chemical agents, we used a Hoechst 33258 dye uptake assay, which assesses cuticle permeability (Hirani *et al.* 2016). We found that cuticle permeability for dye uptake was increased in all tested *vglu-2* mutant alleles (Figure 6D). However, *vglu-2* mutants did not display an altered response to hypertonic stress (Figure 6E), a stressor that depends on cuticle integrity as well (Dodd *et al.* 2018). To assess ultrastructural features of the cuticle of the *vglu-2* mutant, we

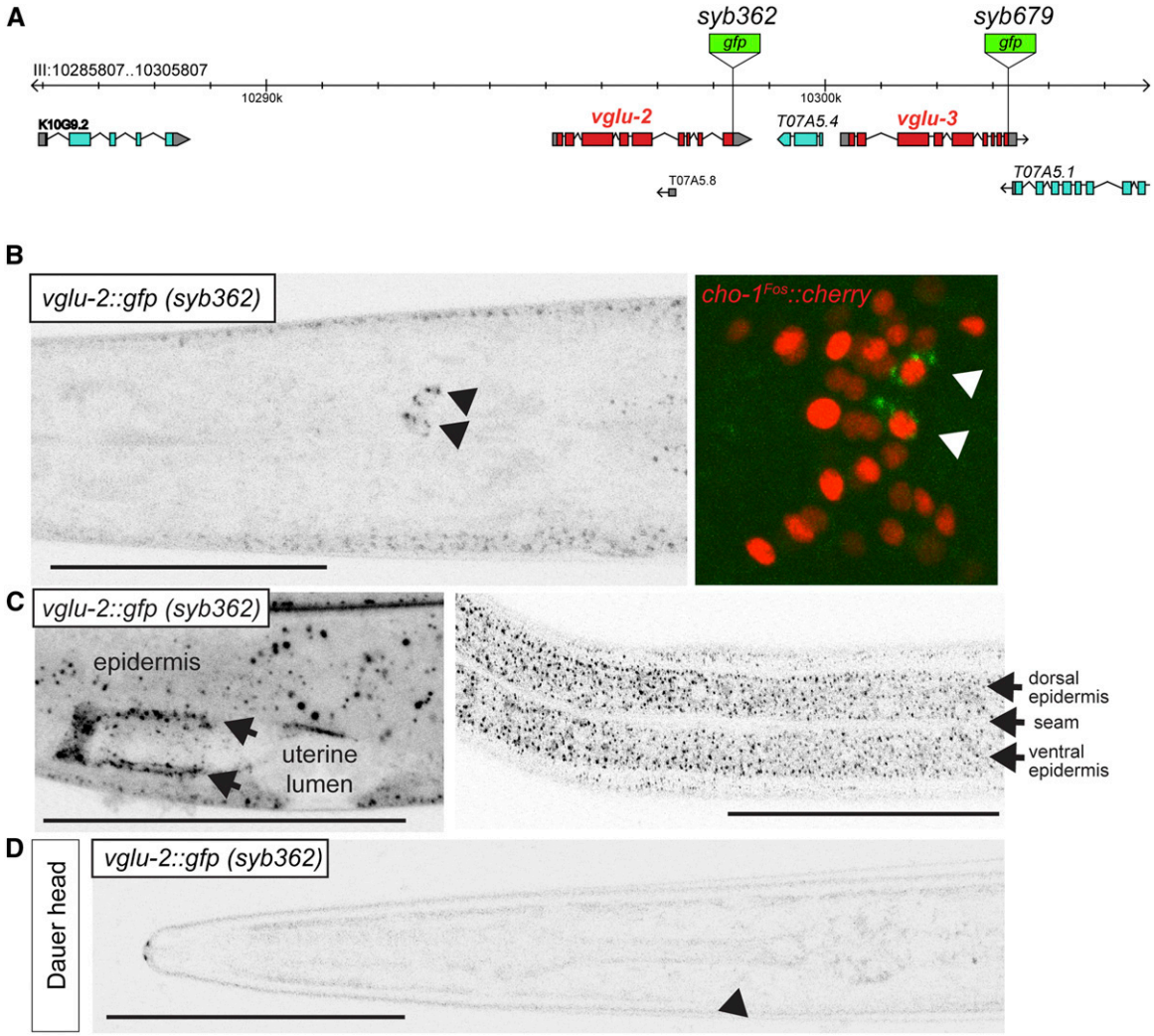

Figure 4 Expression and localization patterns of *vglu-2* in the nervous system. (A) Schematic of *vglu-2* reporter *vglu-3* loci and location of the *gfp* cassettes generated by CRISPR/Cas9 genome engineering. (B–D) GFP expression in the *vglu-2(syb362[vglu-2::gfp])* strain. (B) Ventral view of a young adult animal, showing neuronal, punctate expression in AIA neurons (marked with black arrowhead). AIA identity was confirmed by crossing reporter with AIA-expressed, nuclear-localized *cho-1* reporter (right panel; red signal). Green signal in right panel is VGLU-2::GFP (marked with arrows). (C) Nonneuronal expression in epidermis and uterine tissue lining the uterine lumen (arrows). (D) Lateral view of a dauer-stage animal. Black arrowhead indicates approximate position of AIA, in which VGLU-2::GFP is downregulated, as it is in the epidermis. Bar, 50 μm.

examined the localization of two cuticular proteins, the cuticle collagen COL-19 (Liu *et al.* 1995) and the hedgehog-related protein QUA-1 (Hao *et al.* 2006), but observed no obvious defects (Figure S3). In conclusion, our results indicate that *vglu-2* is involved in ensuring proper cuticle integrity and permeability.

vglu-2 mutants are defective in AIA-dependent responses to odor

C. elegans navigates toward attractive odors using a biased random-walk strategy, for which odor addition suppresses reorientations and odor removal increases reorientation rate (Pierce-Shimomura *et al.* 1999). The *vglu-2*-expressing AIA interneurons are activated by odor addition, and contribute both to the suppression of reorientations and their increase after odor removal (Larsch *et al.* 2015). To ask whether *vglu-2* is important in this function, we monitored the behavioral responses of freely moving animals exposed to diacetyl pulses in microfluidic devices (Figure 7, A and B and Figure S4, *Materials and Methods*). Concentration-dependent induction of reorientation was observed after the removal of 115 nM diacetyl, with larger magnitude responses at diacetyl concentrations $\geq$ 1 μM (Figure 7, A and B). In animals in which AIA interneurons were silenced by expression of the hyperactive potassium channel *unc-103(gf)* under an AIA-specific promoter (Larsch *et al.* 2015), odor-evoked reversals were observed only after removal of the highest concentration, 11 μM (Figure 7, A and B). *vglu-2* mutants had similar, but less severe, behavioral defects in their diacetyl responses at intermediate concentrations (Figure 7, A and B). These defects were rescued in transgenic animals in which the *vglu-2* genomic locus was expressed under an AIA-specific

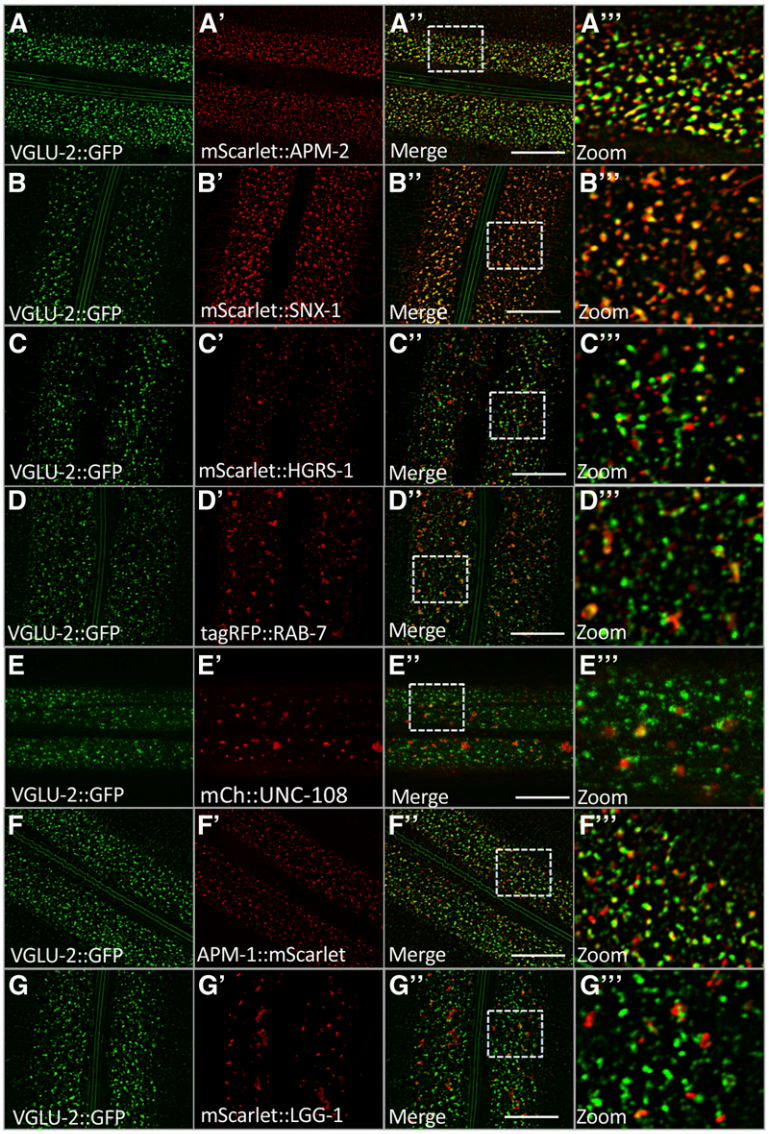

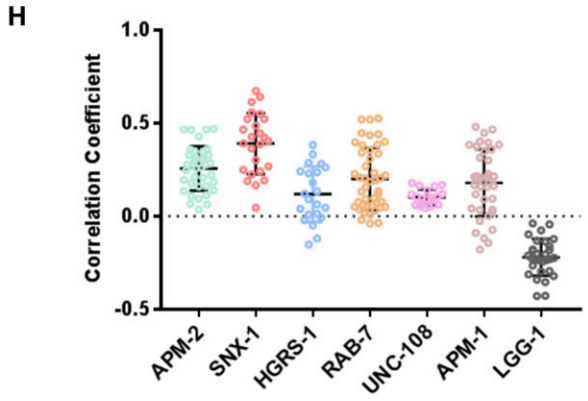

Figure 5 Colocalization of VGLU-2 with organelle-specific markers. (A–G) Images of VGLU-2::GFP colocalization with markers are from deconvolved three-dimensional confocal image stacks acquired in intact living animals expressing VGLU-2::GFP *(syb362)* and red-tagged proteins specifically in hypodermal epithelial cells. (A–A'') VGLU-2::GFP colocalizes with a fraction of apical clathrin-coated pits marked with mScarlet::APM-2. (A''') Magnified image of (A'') is designated by rectangular outline. (B–B'') VGLU-2::GFP colocalizes extensively with mScarlet::SNX-1, a marker for the recycling microdomain of early endosomes. (B''') Magnified image of B'' is designated by rectangular outline. (C–C'') VGLU-2::GFP colocalizes to a lesser degree with mScarlet::HGRS-1, a marker for the degradative microdomain of early endosomes. (C''') Magnified image of (C'') is designated by rectangular outline. (D–D'') VGLU-2::GFP colocalizes to a lesser degree with tagRFP::RAB-7, a marker for late endosomes and lysosomes. (D''') Magnified image of (D'') is designated by rectangular outline. (E–E'') VGLU-2::GFP colocalizes to a very small degree with mCherry::UNC-108. (E''') Magnified image of (E'') is designated by rectangular outline. (F–F'') VGLU-2::GFP colocalizes to a lesser degree with APM-1::mScarlet, a marker for the *trans*-Golgi network. (F''') Magnified image of (F'') is designated by rectangular outline. (G–G'') VGLU-2::GFP fails to colocalize with mScarlet::LGG-1, a marker for autophagosomes. (G''') Magnified image of (G'') is designated by rectangular outline. Bar, 10 μm. (H) Pearson's correlation coefficient measurements for colocalization of VGLU-2::GFP with red fluorescent organellar markers.

promoter (Figure 7, A and B). Thus, *vglu-2* contributes to AIA function in odor-induced behaviors.

Regulation of vglu-2 expression in AIA

The highly selective expression of *vglu-2* in the nervous system prompted us to ask how *vglu-2* expression is regulated. A promoter fusion that contains 2-kb of sequences upstream of *vglu-2* showed a similar expression pattern to the *gfp*-tagged endogenous locus, including the recapitulation of the expression in the AIA interneurons (Figure 8A). Like the *gfp*-tagged endogenous locus, expression of this reporter construct was also downregulated in the dauer

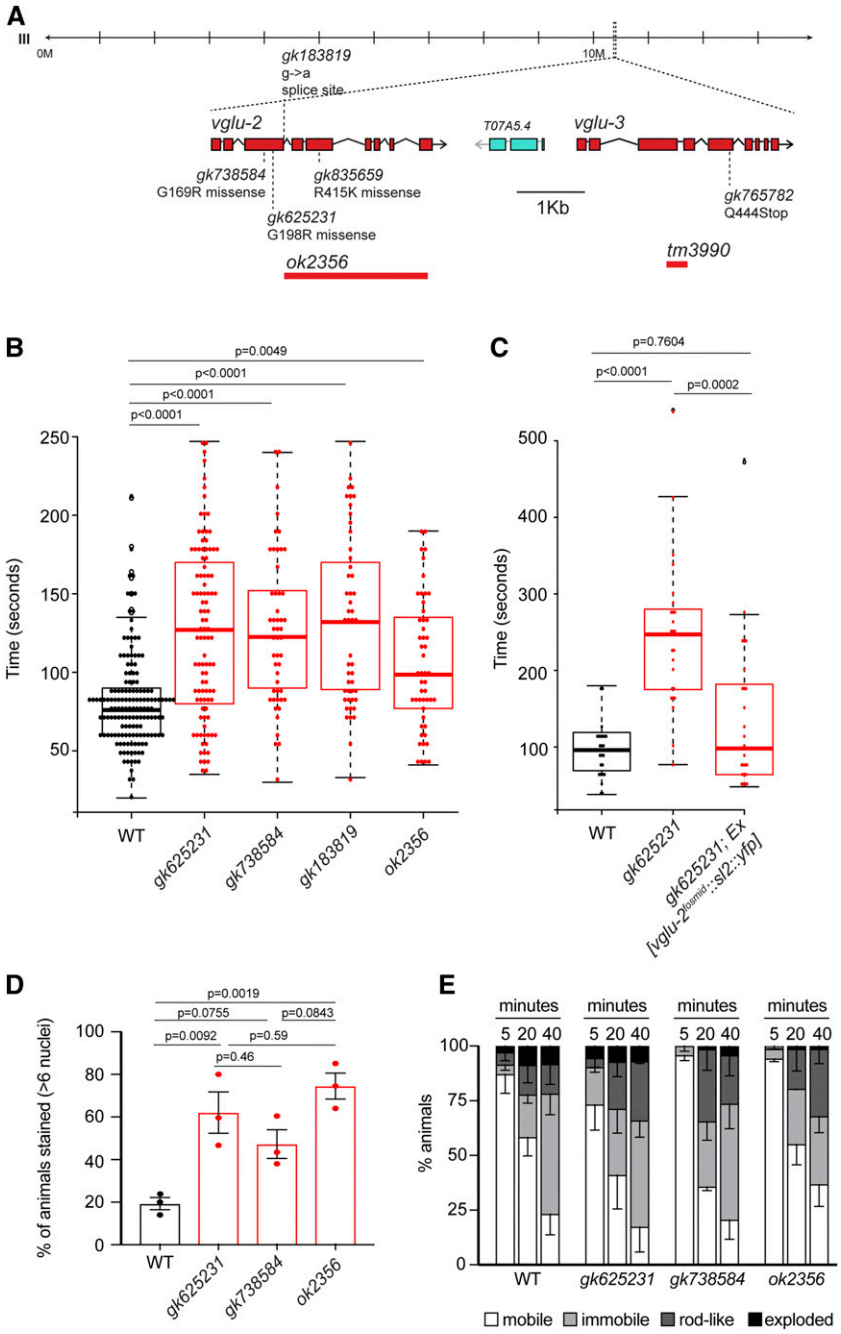

Figure 6 Cuticle defects in *vglu-2* mutants. (A) Genomic locus of *vglu-2* and *vglu-3* including analyzed mutant alleles. (B) *vglu-2* mutant cuticle is more resistant to alkaline bleach-mediated disintegration. The graphs indicate the time (seconds) for cuticle disintegration in alkaline bleach, scored for the first major break in the worm cuticle. (C) The higher resistance to alkaline bleach treatment was rescued in *vglu-2(gk625231)* mutants injected with the *vglu-2* fosmid. For (B, C), statistical significance was determined using the Kruskal–Wallis test followed by Dunn's test for multiple comparisons. No statistically significant changes ($P > 0.05$) between the different *vglu-2* mutants were detected. (D) *vglu-2* mutants display cuticle barrier defects. Values are displayed as mean ± SEM from three independent experiments (each represented as one data point; $n = 50$ per experiment and genotype). For all assays, statistical significance was determined using one-way ANOVA followed by a *post hoc* Tukey test for multiple comparisons. No statistically significant changes ($P > 0.05$) between the different *vglu-2* mutants were detected. (E) Hypoosmotic sensitivity is unaffected in *vglu-2* mutants. The behavior of 2-day old animals was scored as "mobile" (white), "immobile" (light gray), "rod-like" (dark gray), or "exploded" (black), 5, 20, and 40 min following their transfer to distilled water. For each time point, the percentage of animals in each of these states is expressed as mean ± SEM from three independent experiments. WT, wild-type.

stage, indicating that this plasticity is regulated at the transcriptional level. Previous dissection of the *cis*-regulatory control regions of several AIA-expressed genes has shown that expression in the AIA interneurons requires two *cis*-regulatory motifs (Zhang *et al.* 2014). We found that the 2-kb upstream region of *vglu-2* indeed contains these motifs (Figure 8A). One of these motifs was previously found to bind the TTX-3 LIM homeodomain transcription factor, a terminal selector of AIA neuron identity (Zhang *et al.* 2014). We found that *vglu-2* expression was abrogated in the AIA neurons of *ttx-3* null mutants (Figure 8B). This finding corroborates the function of *ttx-3* as a regulator of AIA identity.

Analysis of vglu-3 expression and function

Animals that carry the *gfp*-tagged *vglu-3* allele failed to show *gfp* expression at any developmental stage in both sexes in any tissue type. Attempts to detect low levels of expression by anti-GFP antibody staining also failed. We also failed to observe expression of the transcriptional *vglu-3* fosmid-based reporter construct in which the reporter cassette was separated from *vglu-3* with an SL2 *trans*-splicing sequence, thereby constituting a transcriptional reporter (and avoiding issues such as destabilization of the protein via the addition of the *gfp* reporter). None of five transgenic lines displayed any expression. We also note that whole-animal transcriptome

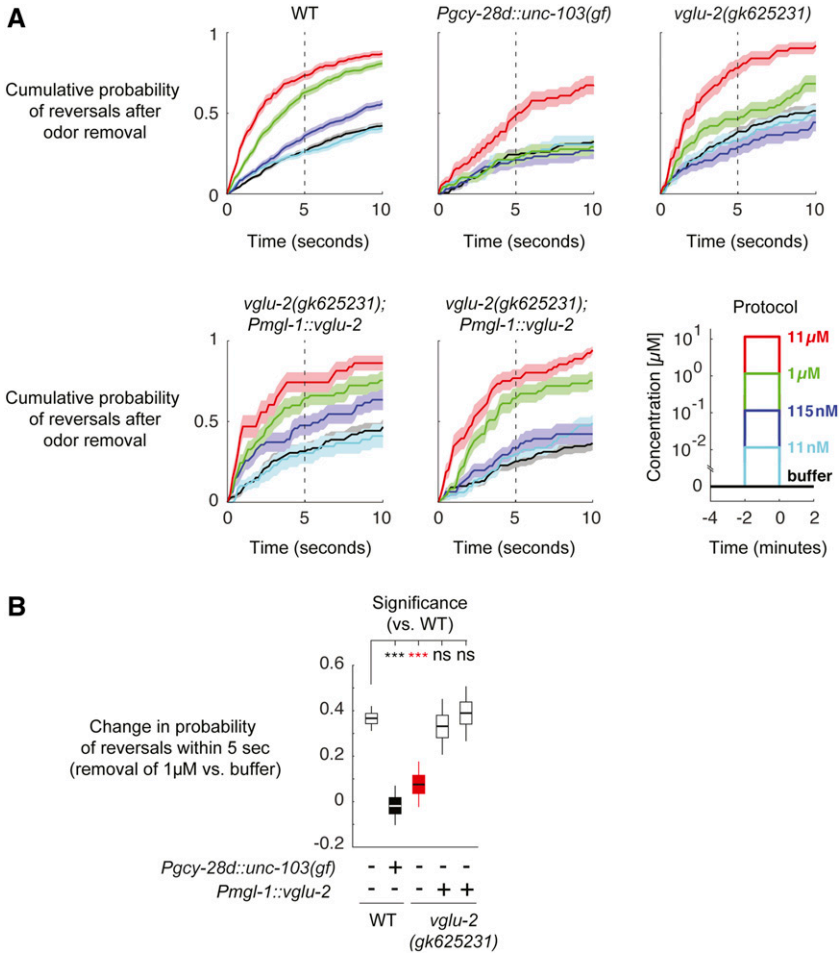

Figure 7 *vglu-2* expression in AIA is required for normal induction of reversals in response to diacetyl removal. (A) Animals freely moving in microfluidic devices were exposed to various diacetyl concentrations (lower-right panel, $t < 0$). The cumulative probability of reversal initiation in response to diacetyl removal ($t > 0$) was quantified (mean + SD). (B) Change in cumulative probability of initiating reversals within 5 sec after 1 μM diacetyl removal relative to the buffer–buffer transition probability (control). Significance was calculated by bootstrap with false discovery rate correction for multiple hypotheses (genotypes). *** $P < 5 \times 10^{-5}$. Similar results were obtained using the Kolmogorov–Smirnov test (*Materials and Methods*). Shown statistics: median (horizontal lines), 25th to 75th percentiles (boxes), and 5th to 95th percentiles (vertical lines). Number of animals (repeats): N2, 226 (678); *Pgcy-28d::unc-103(gf)*, 44 (132); *vglu-2(gk625231)*, 60 (180); *vglu-2(gk625231);Pmgl-1::vglu-2* (OH16032), and 46 (138); *vglu-2(gk625231);Pmgl-1::vglu-2* (OH16031), 45 (135). See Figure S4 for full results. ns, not significant; WT, wild-type.

sequencing by the Model Organism ENCyclopedia Of DNA Elements project (Gerstein *et al.* 2010) revealed very few reads for *vglu-3* under all conditions tested (< 10 fragments per kilobase of transcript per million mapped reads), about an order of magnitude less than for *vglu-2*. However, very low levels of *vglu-3* transcript were previously found in transcriptome profiling of sperm (Ebbing *et al.* 2018). In light of the expression of mammalian *VGLUT* genes in spermatids (Hayashi *et al.* 2003), we therefore tested the remote possibility that very low *vglu-3* expression in sperm may be required for sperm function or fertility. We first measured the brood size of *vglu-3(tm3990)* and *vglu-3(gk765782)* mutants, both likely null mutants (deletion and nonsense allele; Figure 6A). Hermaphrodites from both mutant strains produce comparable numbers of progeny to wild-type N2 (see *Materials and Methods*). We also examined male sperm from *vglu-3* mutants. Spermatids from *C. elegans* are round-shaped and before fertilization they are activated into polarized, motile spermatozoa with pseudopods. This activation process can take place *in vitro* in the presence of pronase or several other reagents (Ward *et al.* 1983). Spermatids from both *vglu-3* mutant alleles display normal morphologies and can also activate in pronase, similar to the control (see *Materials and Methods*). These results suggest that spermatogenesis in *vglu-3* mutants is probably normal. Taken together, our inability to detect expression or a mutant phenotype of *vglu-3* suggests that, after creation through a *C. elegans*-specific gene duplication event of the more ancestral *vglu-2* gene, *vglu-3* may not have maintained any noticeable expression. This could be related to the insertion of the T07A5.4 gene just upstream of *vglu-3* (Figure 3B), which (like *vglu-3* itself) was also generated by a *C. elegans*-specific duplication event that originated from the highly conserved F37C4.5 gene, located on a different chromosome.

Discussion

The original impetus for this study was to assign neurotransmitter identities to *C. elegans* neurons with no previously identified neurotransmitter. Since the complete set of vertebrate glutamatergic neurons is defined by the expression of multiple distinct VGLUT genes (Liguz-Lecznar and Skangiel-Kramska 2007), we considered *vglu-2* and *vglu-3* to be the most obvious candidates to reveal novel glutamatergic neurons. However, our analysis of *vglu-2* and *vglu-3* failed to assign a glutamatergic neurotransmitter identity to neurons that previously had no neurotransmitter identity assigned. Only a single neuron was found to express either of these

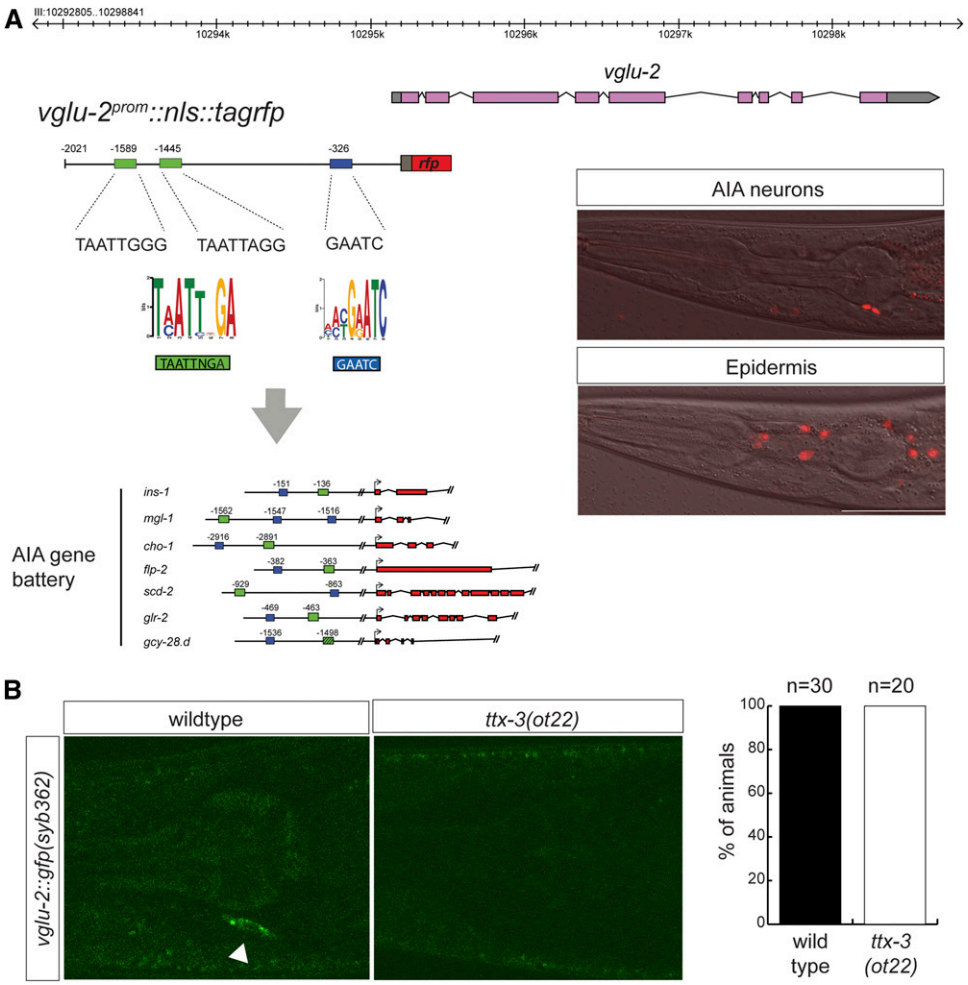

Figure 8 Control of *vglu-2* gene expression in the nervous system. (A) *vglu-2* transcriptional reporter contains putative *cis*-regulatory motifs found in other AIA-expressed genes (Zhang *et al.* 2014). This nuclear-localized reporter recapitulates expression in the two AIA neurons (upper panel) and epidermis (lower panel; different plane of focus). (B) Expression of *vglu-2* transcriptional reporter in AIA in wild-type and *ttx-3(ot22)* mutant animals. Bar, 50 μm. rfp, red fluorescent protein.

two genes and this neuron, AIA, already had a previously assigned cholinergic transmitter identity (Altun-Gultekin *et al.* 2001; Pereira *et al.* 2015). *vglu-3* did not show any detectable expression in the nervous system (or in any other tissue type). Since there are no additional obvious VGLUT sequence homologs encoded in the genome, it appears that the previous assignment of glutamatergic identity by expression of *eat-4/VGLUT* (Serrano-Saiz *et al.* 2013, 2017) probably identified all glutamatergic neurons in the *C. elegans* nervous system. However, we caution that: (1) very low, but nevertheless functionally relevant, levels of *eat-4*, *vglu-2*, or *vglu-3* expression may have escaped detection, and (2) it cannot be completely excluded that *C. elegans* members of the SCL17A5/Sialin subfamily (Figure 1A) may constitute vesicular glutamate transporters. Even though primarily localized to lysosomes, vertebrate SCL17A5/Sialin (a sialic acid transporter) may also have the potential to be a vesicular transporter for aspartate and glutamate (Aula *et al.* 2004; Miyaji *et al.* 2008), but the *in vivo* relevance of these biochemical activities is controversial (Morland *et al.* 2013; Herring *et al.* 2015).

While we observed GFP-tagged VGLU-2 to localize to vesicles in the soma of the AIA neurons, we did not observe these vesicles to cluster along AIA axons, as one may expect from a synaptic vesicular transporter. Therefore, it remains unclear whether VGLU-2 acts as a synaptic Glu transporter in AIA. However, our analysis of VGLU-2 in the epidermis indicates that VGLU-2 may have a role in endosomal trafficking. While we refrain from speculating about the function of VGLU-2 in AIA neurons, some possible functions can be inferred for epidermal VGLU-2 based on described functions of vertebrate VGLUT1 in osteoclasts. Osteoclasts are localized next to bone and are required for bone resorption. In these large multinucleate cells, VGLUT1 localizes to transcytotic vesicles (Morimoto *et al.* 2006). Bone resorption apparently depends on glutamate-loaded transcytotic vesicles in osteoclasts that are thought to transport bone degradation products, including collagens (Morimoto *et al.* 2006). VGLUT1 controls the secretion of these transcytotic vesicles via an autocrine, Glu release-dependent mechanism (Morimoto *et al.* 2006). The *C. elegans* epidermis also displays high intracellular transport activity, required to control the synthesis and breakdown of the collagen-containing cuticle (Chisholm and Xu 2012). Hence, based on the vertebrate VGLUT1 precedent, we hypothesize that vesicularly localized VGLU-2 may have a role in some aspect of cuticular collagen endocytosis and

trafficking, perhaps even transcytosis. Consistent with a speculative role of VGLU-2 in cuticle collagen turnover in *C. elegans*, we find that *vglu-2* mutants display an altered sensitivity to sodium hypochlorite, which is known to break down collagens. It is easy to envision that alteration in the collagen matrix could affect the barrier function of the cuticle, as exemplified by the altered dye uptake of *vglu-2* mutants.

In light of the downregulation and redistribution of VGLU-2::GFP in dauers, it is notable that animals that enter the dauer arrest stage substantially remodel their cuticle and collagen composition (Cox *et al.* 1981; Cox and Hirsh 1985; Kramer *et al.* 1985; Lee *et al.* 2017; Shih *et al.* 2019). VGLU-2 expression changes may be required for these remodeling events. Additional studies are required to understand how *vglu-2* controls cuticle integrity.

Acknowledgments

We thank Chi Chen for generating transgenic strains, Nathalie Pujol and Michel Labouesse for providing the *vha-5* reporter strain, Xiaochen Wang for the *unc-108* reporter strain, James Rand for communicating the analysis of his search of *vglu* genes in *C. inopinata*, and the *Caenorhabditis* Genetics Center (CGC) [supported by the National Institutes of Health (NIH) Office of Research Infrastructure Programs (P40 OD-010440)] and the National Bioresource Project for the Nematode (directed by Shohei Mitani at Tokyo Women's Medical University School of Medicine) for providing mutant strains. B.D.G. was supported by NIH grant R01 GM-067237, A.S. and X.M. by NIH grant HD-054681 and O.H. by the Howard Hughes Medical Institute.

Literature Cited

Abrams, T. W., and W. Sossin, 2019 Invertebrate genomics provide insights into the origin of synaptic transmission, in *The Oxford Handbook of Invertebrate Neurobiology*, edited by J. H Byrne. Oxford University Press, Oxford.

Adler, J., and I. Parmryd, 2010 Quantifying colocalization by correlation: the Pearson correlation coefficient is superior to the Mander's overlap coefficient. Cytometry A 77: 733–742. https://doi.org/10.1002/cyto.a.20896

Albrecht, D. R., and C. I. Bargmann, 2011 High-content behavioral analysis of *Caenorhabditis elegans* in precise spatiotemporal chemical environments. Nat. Methods 8: 599–605. https://doi.org/10.1038/nmeth.1630

Alfonso, A., K. Grundahl, J. S. Duerr, H. P. Han, and J. B. Rand, 1993 The Caenorhabditis elegans unc-17 gene: a putative vesicular acetylcholine transporter. Science 261: 617–619. https://doi.org/10.1126/science.8342028

Almqvist, J., Y. Huang, A. Laaksonen, D. N. Wang, and S. Hovmoller, 2007 Docking and homology modeling explain inhibition of the human vesicular glutamate transporters. Protein Sci. 16: 1819–1829. https://doi.org/10.1110/ps.072944707

Altun-Gultekin, Z., Y. Andachi, E. L. Tsalik, D. Pilgrim, Y. Kohara *et al.*, 2001 A regulatory cascade of three homeobox genes, ceh-10, ttx-3 and ceh-23, controls cell fate specification of a defined interneuron class in *C. elegans*. Development 128: 1951–1969.

Aula, N., O. Kopra, A. Jalanko, and L. Peltonen, 2004 Sialin expression in the CNS implicates extralysosomal function in neurons. Neurobiol. Dis. 15: 251–261. https://doi.org/10.1016/j.nbd.2003.11.017

Blaxter, M. L., P. De Ley, J. R. Garey, L. X. Liu, P. Scheldeman *et al.*, 1998 A molecular evolutionary framework for the phylum Nematoda. Nature 392: 71–75. https://doi.org/10.1038/32160

C. elegans Deletion Mutant Consortium, 2012 Large-scale screening for targeted knockouts in the Caenorhabditis elegans genome. G3 (Bethesda) 2: 1415–1425.

Chatterjee, I., C. Ibanez-Ventoso, P. Vijay, G. Singaravelu, C. Baldi *et al.*, 2013 Dramatic fertility decline in aging *C. elegans* males is associated with mating execution deficits rather than diminished sperm quality. Exp. Gerontol. 48: 1156–1166. https://doi.org/10.1016/j.exger.2013.07.014

Chisholm, A. D., and S. Xu, 2012 The Caenorhabditis elegans epidermis as a model skin. II: differentiation and physiological roles. Wiley Interdiscip. Rev. Dev. Biol. 1: 879–902. https://doi.org/10.1002/wdev.77

Chronis, N., M. Zimmer, and C. I. Bargmann, 2007 Microfluidics for in vivo imaging of neuronal and behavioral activity in Caenorhabditis elegans. Nat. Methods 4: 727–731. https://doi.org/10.1038/nmeth1075

Cox, G. N., and D. Hirsh, 1985 Stage-specific patterns of collagen gene expression during development of Caenorhabditis elegans. Mol. Cell. Biol. 5: 363–372. https://doi.org/10.1128/MCB.5.2.363

Cox, G. N., S. Staprans, and R. S. Edgar, 1981 The cuticle of Caenorhabditis elegans. II. Stage-specific changes in ultrastructure and protein composition during postembryonic development. Dev. Biol. 86: 456–470. https://doi.org/10.1016/0012-1606(81)90204-9

Daniels, R. W., C. A. Collins, M. V. Gelfand, J. Dant, E. S. Brooks *et al.*, 2004 Increased expression of the Drosophila vesicular glutamate transporter leads to excess glutamate release and a compensatory decrease in quantal content. J. Neurosci. 24: 10466–10474. https://doi.org/10.1523/JNEUROSCI.3001-04.2004

Davies, J. M., D. A. Horwitz, and K. J. Davies, 1993 Potential roles of hypochlorous acid and N-chloroamines in collagen breakdown by phagocytic cells in synovitis. Free Radic. Biol. Med. 15: 637–643. https://doi.org/10.1016/0891-5849(93)90167-S

Dickinson, D. J., A. M. Pani, J. K. Heppert, C. D. Higgins, and B. Goldstein, 2015 Streamlined genome engineering with a self-excising drug selection cassette. Genetics 200: 1035–1049. https://doi.org/10.1534/genetics.115.178335

Dierking, K., J. Polanowska, S. Omi, I. Engelmann, M. Gut *et al.*, 2011 Unusual regulation of a STAT protein by an SLC6 family transporter in *C. elegans* epidermal innate immunity. Cell Host Microbe 9: 425–435. https://doi.org/10.1016/j.chom.2011.04.011

Dodd, W., L. Tang, J. C. Lone, K. Wimberly, C. W. Wu *et al.*, 2018 A damage sensor associated with the cuticle coordinates three core environmental stress responses in Caenorhabditis elegans. Genetics 208: 1467–1482. https://doi.org/10.1534/genetics.118.300827

Duerr, J. S., D. L. Frisby, J. Gaskin, A. Duke, K. Asermely *et al.*, 1999 The cat-1 gene of Caenorhabditis elegans encodes a vesicular monoamine transporter required for specific monoamine-dependent behaviors. J. Neurosci. 19: 72–84. https://doi.org/10.1523/JNEUROSCI.19-01-00072.1999

Duerr, J. S., J. Gaskin, and J. B. Rand, 2001 Identified neurons in *C. elegans* coexpress vesicular transporters for acetylcholine and monoamines. Am. J. Physiol. Cell Physiol. 280: C1616–C1622. https://doi.org/10.1152/ajpcell.2001.280.6.C1616

Ebbing, A., A. Vertesy, M. C. Betist, B. Spanjaard, J. P. Junker *et al.*, 2018 Spatial transcriptomics of *C. elegans* males and hermaphrodites identifies sex-specific differences in gene expression patterns. Dev. Cell 47: 801–813.e6.

El Mouridi, S., C. Lecroisey, P. Tardy, M. Mercier, A. Leclercq-Blondel *et al.*, 2017 Reliable CRISPR/Cas9 genome engineering in

Caenorhabditis elegans using a single efficient sgRNA and an easily recognizable phenotype. G3 (Bethesda) 7: 1429–1437. https://doi.org/10.1534/g3.117.040824

Félix, M. A., C. Braendle, and A. D. Cutter, 2014 A streamlined system for species diagnosis in Caenorhabditis (Nematoda: Rhabditidae) with name designations for 15 distinct biological species. PLoS One 9: e94723 [corrigenda: PLoS One 10: e0118327 (2015)]. https://doi.org/10.1371/journal.pone.0094723

Frøkjær-Jensen, C., M. W. Davis, M. Sarov, J. Taylor, S. Flibotte *et al*., 2014 Random and targeted transgene insertion in Caenorhabditis elegans using a modified Mos1 transposon. Nat. Methods 11: 529–534. https://doi.org/10.1038/nmeth.2889

Geldziler, B. D., M. R. Marcello, D. C. Shakes, and A. Singson, 2011 The genetics and cell biology of fertilization. Methods Cell Biol. 106: 343–375. https://doi.org/10.1016/B978-0-12-544172-8.00013-X

Gendrel, M., E. G. Atlas, and O. Hobert, 2016 A cellular and regulatory map of the GABAergic nervous system of *C. elegans*. Elife 5: e17686. https://doi.org/10.7554/eLife.17686

Gerstein, M. B., Z. J. Lu, E. L. Van Nostrand, C. Cheng, B. I. Arshinoff *et al*., 2010 Integrative analysis of the Caenorhabditis elegans genome by the modENCODE project. Science 330: 1775–1787. https://doi.org/10.1126/science.1196914

Gras, C., E. Herzog, G. C. Bellenchi, V. Bernard, P. Ravassard *et al*., 2002 A third vesicular glutamate transporter expressed by cholinergic and serotoninergic neurons. J. Neurosci. 22: 5442–5451. https://doi.org/10.1523/JNEUROSCI.22-13-05442.2002

Hao, L., K. Mukherjee, S. Liegeois, D. Baillie, M. Labouesse *et al*., 2006 The hedgehog-related gene qua-1 is required for molting in Caenorhabditis elegans. Dev. Dyn. 235: 1469–1481. https://doi.org/10.1002/dvdy.20721

Hayashi, M., R. Morimoto, A. Yamamoto, and Y. Moriyama, 2003 Expression and localization of vesicular glutamate transporters in pancreatic islets, upper gastrointestinal tract, and testis. J. Histochem. Cytochem. 51: 1375–1390. https://doi.org/10.1177/002215540305101014

Hediger, M. A., M. F. Romero, J. B. Peng, A. Rolfs, H. Takanaga *et al*., 2004 The ABCs of solute carriers: physiological, pathological and therapeutic implications of human membrane transport proteinsIntroduction. Pflugers Arch. 447: 465–468. https://doi.org/10.1007/s00424-003-1192-y

Herring, B. E., K. Silm, R. H. Edwards, and R. A. Nicoll, 2015 Is aspartate an excitatory neurotransmitter? J. Neurosci. 35: 10168–10171. https://doi.org/10.1523/JNEUROSCI.0524-15.2015

Hirani, N., M. Westenberg, P. T. Seed, M. I. Petalcorin, and C. T. Dolphin, 2016 *C. elegans* flavin-containing monooxygenase-4 is essential for osmoregulation in hypotonic stress. Biol. Open 5: 537–549. https://doi.org/10.1242/bio.017400

Hobert, O., 2013 The neuronal genome of *Caenorhabditis elegans* (August 13, 2013), WormBook, ed. The *C. elegans* Research Community, WormBook, doi/10.1895/wormbook.1.161.1, http://www.wormbook.org. https://doi.org/10.1895/wormbook.1.161.1

Höglund, P. J., K. J. Nordström, H. B. Schiöth, and R. Fredriksson, 2011 The solute carrier families have a remarkably long evolutionary history with the majority of the human families present before divergence of Bilaterian species. Mol. Biol. Evol. 28: 1531–1541. https://doi.org/10.1093/molbev/msq350

Horie, T., T. Kusakabe, and M. Tsuda, 2008 Glutamatergic networks in the Ciona intestinalis larva. J. Comp. Neurol. 508: 249–263. https://doi.org/10.1002/cne.21678

Johnstone, I. L., 2000 Cuticle collagen genes. Expression in Caenorhabditis elegans. Trends Genet. 16: 21–27. https://doi.org/10.1016/S0168-9525(99)01857-0

Kanzaki, N., I. J. Tsai, R. Tanaka, V. L. Hunt, D. Liu *et al*., 2018 Biology and genome of a newly discovered sibling species of Caenorhabditis elegans. Nat. Commun. 9: 3216. https://doi.org/10.1038/s41467-018-05712-5

Köhnlein, K., N. Urban, D. Guerrero-Gómez, H. Steinbrenner, P. Urbánek *et al*., 2019 A Caenorhabditis elegans ortholog of human selenium-binding protein 1 is a pro-aging factor protecting against selenite toxicity. Redox Biol. 28: 101323. https://doi.org/10.1016/j.redox.2019.101323

Kramer, J. M., G. N. Cox, and D. Hirsh, 1985 Expression of the Caenorhabditis elegans collagen genes col-1 and col-2 is developmentally regulated. J. Biol. Chem. 260: 1945–1951.

Larsch, J., S. W. Flavell, Q. Liu, A. Gordus, D. R. Albrecht *et al*., 2015 A circuit for gradient climbing in *C. elegans* chemotaxis. Cell Rep. 12: 1748–1760. https://doi.org/10.1016/j.celrep.2015.08.032

Lee, D., S. Jung, J. Ryu, J. Ahnn, and I. Ha, 2008 Human vesicular glutamate transporters functionally complement EAT-4 in *C. elegans*. Mol. Cells 25: 50–54.

Lee, J. S., P. Y. Shih, O. N. Schaedel, P. Quintero-Cadena, A. K. Rogers *et al*., 2017 FMRFamide-like peptides expand the behavioral repertoire of a densely connected nervous system. Proc. Natl. Acad. Sci. USA 114: E10726–E10735. https://doi.org/10.1073/pnas.1710374114

Lee, R. Y., E. R. Sawin, M. Chalfie, H. R. Horvitz, and L. Avery, 1999 EAT-4, a homolog of a mammalian sodium-dependent inorganic phosphate cotransporter, is necessary for glutamatergic neurotransmission in caenorhabditis elegans. J. Neurosci. 19: 159–167. https://doi.org/10.1523/JNEUROSCI.19-01-00159.1999

Levy, S., and C. I. Bargmann, 2019 An adaptive-threshold mechanism for odor sensation and animal navigation. Neuron. https://doi.org/10.1016/j.neuron.2019.10.034

Liégeois, S., A. Benedetto, J. M. Garnier, Y. Schwab, and M. Labouesse, 2006 The V0-ATPase mediates apical secretion of exosomes containing Hedgehog-related proteins in Caenorhabditis elegans. J. Cell Biol. 173: 949–961. https://doi.org/10.1083/jcb.200511072

Liguz-Lecznar, M., and J. Skangiel-Kramska, 2007 Vesicular glutamate transporters (VGLUTs): the three musketeers of glutamatergic system. Acta Neurobiol. Exp. (Warsz.) 67: 207–218.

Liu, Z., S. Kirch, and V. Ambros, 1995 The Caenorhabditis elegans heterochronic gene pathway controls stage-specific transcription of collagen genes. Development 121: 2471–2478.

Loer, C. M., A. C. Calvo, K. Watschinger, G. Werner-Felmayer, D. O'Rourke *et al*., 2015 Cuticle integrity and biogenic amine synthesis in Caenorhabditis elegans require the cofactor tetrahydrobiopterin (BH4). Genetics 200: 237–253. https://doi.org/10.1534/genetics.114.174110

Lu, Q., Y. Zhang, T. Hu, P. Guo, W. Li *et al*., 2008 *C. elegans* Rab GTPase 2 is required for the degradation of apoptotic cells. Development 135: 1069–1080. https://doi.org/10.1242/dev.016063

Manders, E. M., J. Stap, G. J. Brakenhoff, R. van Driel, and J. A. Aten, 1992 Dynamics of three-dimensional replication patterns during the S-phase, analysed by double labelling of DNA and confocal microscopy. J. Cell Sci. 103: 857–862.

McIntire, S. L., R. J. Reimer, K. Schuske, R. H. Edwards, and E. M. Jorgensen, 1997 Identification and characterization of the vesicular GABA transporter. Nature 389: 870–876. https://doi.org/10.1038/39908

Miyaji, T., N. Echigo, M. Hiasa, S. Senoh, H. Omote *et al*., 2008 Identification of a vesicular aspartate transporter. Proc. Natl. Acad. Sci. USA 105: 11720–11724. https://doi.org/10.1073/pnas.0804015105

Morimoto, R., S. Uehara, S. Yatsushiro, N. Juge, Z. Hua *et al*., 2006 Secretion of L-glutamate from osteoclasts through transcytosis. EMBO J. 25: 4175–4186. https://doi.org/10.1038/sj.emboj.7601317

Morland, C., K. Nordengen, M. Larsson, L. M. Prolo, Z. Farzampour *et al*., 2013 Vesicular uptake and exocytosis of L-aspartate is independent of sialin. FASEB J. 27: 1264–1274. https://doi.org/10.1096/fj.12-206300

Norris, A., P. Tammineni, S. Wang, J. Gerdes, A. Murr *et al.*, 2017 SNX-1 and RME-8 oppose the assembly of HGRS-1/ESCRT-0 degradative microdomains on endosomes. Proc. Natl. Acad. Sci. USA 114: E307–E316. https://doi.org/10.1073/pnas.1612730114

Olszowski, S., P. Mak, E. Olszowska, and J. Marcinkiewicz, 2003 Collagen type II modification by hypochlorite. Acta Biochim. Pol. 50: 471–479.

Omote, H., T. Miyaji, M. Hiasa, N. Juge, and Y. Moriyama, 2016 Structure, function, and drug interactions of neurotransmitter transporters in the postgenomic era. Annu. Rev. Pharmacol. Toxicol. 56: 385–402. https://doi.org/10.1146/annurev-pharmtox-010814-124816

Oyarzun, A., A. M. Cordero, and M. Whittle, 2002 Immunohistochemical evaluation of the effects of sodium hypochlorite on dentin collagen and glycosaminoglycans. J. Endod. 28: 152–156. https://doi.org/10.1097/00004770-200203000-00002

Pereira, L., P. Kratsios, E. Serrano-Saiz, H. Sheftel, A. E. Mayo *et al.*, 2015 A cellular and regulatory map of the cholinergic nervous system of *C. elegans*. Elife 4: e12432. https://doi.org/10.7554/eLife.12432

Pierce-Shimomura, J. T., T. M. Morse, and S. R. Lockery, 1999 The fundamental role of pirouettes in Caenorhabditis elegans chemotaxis. J. Neurosci. 19: 9557–9569. https://doi.org/10.1523/JNEUROSCI.19-21-09557.1999

Reimer, R. J., 2013 SLC17: a functionally diverse family of organic anion transporters. Mol. Aspects Med. 34: 350–359. https://doi.org/10.1016/j.mam.2012.05.004

Sato, K., A. Norris, M. Sato, and B. D. Grant, 2014 *C. elegans* as a model for membrane traffic (April 25, 2014), WormBook, ed. The *C. elegans* Research Community, WormBook, doi/10.1895/wormbook.1.77.2, http://www.wormbook.org. https://doi.org/10.1895/wormbook.1.77.2

Sawada, K., N. Echigo, N. Juge, T. Miyaji, M. Otsuka *et al.*, 2008 Identification of a vesicular nucleotide transporter. Proc. Natl. Acad. Sci. USA 105: 5683–5686. https://doi.org/10.1073/pnas.0800141105

Serrano-Saiz, E., R. J. Poole, T. Felton, F. Zhang, E. D. de la Cruz *et al.*, 2013 Modular control of glutamatergic neuronal identity in *C. elegans* by distinct homeodomain proteins. Cell 155: 659–673. https://doi.org/10.1016/j.cell.2013.09.052

Serrano-Saiz, E., L. Pereira, M. Gendrel, U. Aghayeva, A. Battacharya *et al.*, 2017 A neurotransmitter atlas of the Caenorhabditis elegans male nervous system reveals sexually dimorphic neurotransmitter usage. Genetics 206: 1251–1269. https://doi.org/10.1534/genetics.117.202127

Shakes, D. C., and S. Ward, 1989 Initiation of spermiogenesis in *C. elegans*: a pharmacological and genetic analysis. Dev. Biol. 134: 189–200. https://doi.org/10.1016/0012-1606(89)90088-2

Shao, Z., S. Watanabe, R. Christensen, E. M. Jorgensen, and D. A. Colon-Ramos, 2013 Synapse location during growth depends on glia location. Cell 154: 337–350. https://doi.org/10.1016/j.cell.2013.06.028

Shih, P. Y., J. S. Lee, and P. W. Sternberg, 2019 Genetic markers enable the verification and manipulation of the dauer entry decision. Dev. Biol. 454: 170–180. https://doi.org/10.1016/j.ydbio.2019.06.009

Singaravelu, G., I. Chatterjee, M. R. Marcello, and A. Singson, 2011 Isolation and in vitro activation of Caenorhabditis elegans sperm. J. Vis. Exp. 47: 2336. https://doi.org/10.3791/2336

Singson, A., K. B. Mercer, and S. W. L'Hernault, 1998 The *C. elegans* spe-9 gene encodes a sperm transmembrane protein that contains EGF-like repeats and is required for fertilization. Cell 93: 71–79. https://doi.org/10.1016/S0092-8674(00)81147-2

Sreedharan, S., J. H. Shaik, P. K. Olszewski, A. S. Levine, H. B. Schioth *et al.*, 2010 Glutamate, aspartate and nucleotide transporters in the SLC17 family form four main phylogenetic clusters: evolution and tissue expression. BMC Genomics 11: 17. https://doi.org/10.1186/1471-2164-11-17

Stiernagle, T., 2006 Maintenance of *C. elegans* (February 11, 2006), WormBook, ed. The *C. elegans* Research Community, WormBook, doi/10.1895/wormbook.1.101.1, http://www.wormbook.org.

Takamori, S., J. S. Rhee, C. Rosenmund, and R. Jahn, 2000 Identification of a vesicular glutamate transporter that defines a glutamatergic phenotype in neurons. Nature 407: 189–194. https://doi.org/10.1038/35025070

Takamori, S., J. S. Rhee, C. Rosenmund, and R. Jahn, 2001 Identification of differentiation-associated brain-specific phosphate transporter as a second vesicular glutamate transporter (VGLUT2). J. Neurosci. 21: RC182. https://doi.org/10.1523/JNEUROSCI.21-22-j0002.2001

Thompson, O., M. Edgley, P. Strasbourger, S. Flibotte, B. Ewing *et al.*, 2013 The million mutation project: a new approach to genetics in Caenorhabditis elegans. Genome Res. 23: 1749–1762. https://doi.org/10.1101/gr.157651.113

Tursun, B., L. Cochella, I. Carrera, and O. Hobert, 2009 A toolkit and robust pipeline for the generation of fosmid-based reporter genes in *C. elegans*. PLoS One 4: e4625. https://doi.org/10.1371/journal.pone.0004625

Ward, S., E. Hogan, and G. A. Nelson, 1983 The initiation of spermiogenesis in the nematode Caenorhabditis elegans. Dev. Biol. 98: 70–79. https://doi.org/10.1016/0012-1606(83)90336-6

Yin, J., Y. Huang, P. Guo, S. Hu, S. Yoshina *et al.*, 2017 GOP-1 promotes apoptotic cell degradation by activating the small GTPase Rab2 in *C. elegans*. J. Cell Biol. 216: 1775–1794. https://doi.org/10.1083/jcb.201610001

Zhang, F., A. Bhattacharya, J. C. Nelson, N. Abe, P. Gordon *et al.*, 2014 The LIM and POU homeobox genes ttx-3 and unc-86 act as terminal selectors in distinct cholinergic and serotonergic neuron types. Development 141: 422–435. https://doi.org/10.1242/dev.099721

Zhang, J., J. Liu, A. Norris, B. D. Grant, and X. Wang, 2018 A novel requirement for ubiquitin-conjugating enzyme UBC-13 in retrograde recycling of MIG-14/Wntless and Wnt signaling. Mol. Biol. Cell 29: 2098–2112. https://doi.org/10.1091/mbc.E17-11-0639

Communicating editor: H. Bülow